U.P.B. Sci. Bull., Series B, Vol. 81, Iss. 3, 2019 ISSN 1454-2331

THE INFLUENCE OF TECHNOLOGICAL PARAMETERS ON THE CHARACTERISTICS OF ARC WELDING DEPOSITIONS

Dumitru-Titi CICIC[1], Gheorghe SOLOMON[2], Theodora Diana DIȚU[3], Corneliu RONTESCU[4], Dan GHEORGHE[5], Gabriel IACOBESCU[6]

The present paper aims at presenting the results obtained following the experiments conducted to determine certain influences of the deposition process parameters - electric current intensity (I_s), electric arc voltage (U_a), deposition speed (v_s) and type of deposition current - on the geometric elements of the deposition such as Width (W), Penetration (P), Reinforcement (R), as well as on dilution (D) and hardness (HV). The arc welding deposition process used during the experiments was robotic Gas Metal Arc Welding (GMAW). The analyzed case was centered on the deposition of a low alloy steel filler material (G3Si1) on a ferritic high alloy steel base material (X6Cr17). The results are presented in charts and tables.

Keywords: arc welding deposition, dilution, ferritic stainless steel

1. Introduction

The term arc welding deposition usually refers to the deposition of a relatively thick layer (≤3 mm) of weld metal in order to provide a corrosion-resistant surface [1].

Usually, these applications imply the manufacture of products out of two different materials - one material should ensure the corrosion resistance and the other one should provide the mechanical properties. If the ferritic high alloy steel layer that should be deposited in order to ensure corrosion resistance is much too thick compared to the resistance layer created by the non-alloy steel, the solution

[1] Associate Professor, Dept. of Materials Technology and Welding, University POLITEHNICA of Bucharest, Romania.
[2] Professor, Dept. of Materials Technology and Welding, University POLITEHNICA of Bucharest, Romania.
[3] Eng. Dept. of Materials Technology and Welding, University POLITEHNICA of Bucharest, Romania.
[4] Associate Professor, Dept. of Materials Technology and Welding, University POLITEHNICA of Bucharest, Romania, e-mail: corneliu.rontescu@upb.ro.
[5] Associate Professor, Dept. of Science of Metal Materials, University POLITEHNICA of Bucharest, Romania.
[6] Professor, Dept. of Materials Technology and Welding, University POLITEHNICA of Bucharest, Romania.

is to choose the alternative of depositing the non-alloy steel on a high alloy steel base material.

The main industrial fields where overlay welding is used are [2-4]: nuclear industry, chemical industry, mining industry, oil industry, shipbuilding industry, etc. The working environments in these industries are highly corrosive leading to high corrosion rates that might determine the operational failure of the products before the expiry of their normal service life. In order to make the product wall thicker thus increasing its resistance to high pressure conditions, it is possible to resort to the technological measure of depositing a carbon steel layer in the area not subjected to corrosion; this measure should provide higher resistance characteristics.

The main arc welding deposition processes are [5, 6]:

- Submerged Arc Welding (SAW);
- Gas Tungsten Arc Welding (GTAW);
- Shielded Metal Arc Welding (SMAW);
- Gas Tungsten Arc Welding Pulsed (GTAW Pulsed);
- Flux Covered Arc Welding (FCAW).

The main geometric elements of arc welding deposition are presented in Fig. 1.

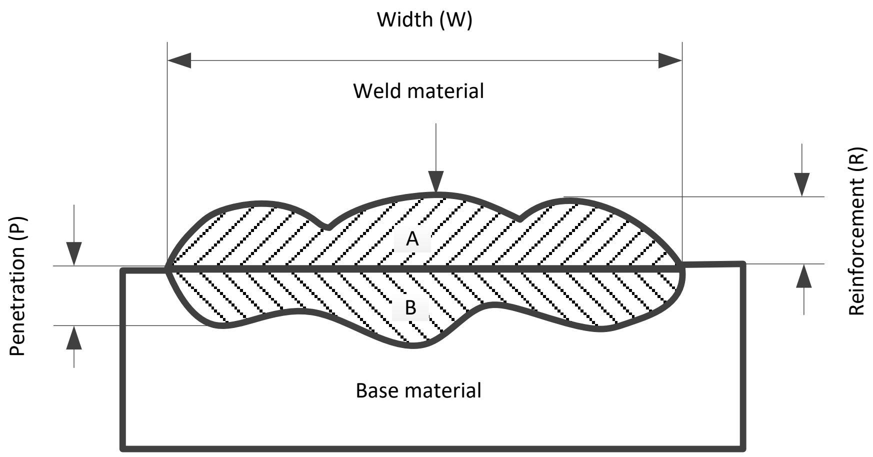

Fig. 1. Characteristic geometric elements of arc welding deposition [7]

According to Fig. 1, one can state that the material of the deposited seam is the result of the base and filler materials being blended together in liquid state, after having melted due to the heat released by the electric arc that was generated during the arc welding deposition.

In order to determine the chemical characteristics of the deposition, it is necessary to take into account the chemical compositions of the base and filler materials, the degree of admixture of the two materials, as well as the parameters of the deposition processes. The final composition, the corresponding microstructure and the properties of the fusion zone will be determined by the dilution level [8-12].

Most applications of arc welding deposition refer to the deposition of high alloy (stainless) steel on a base material made of low alloy steel or medium alloy steel.

Following the design of industrial products, several aspects are taken into consideration such as corrosion rates, normal service life, product wall thickness, as well as the pressure forces and temperature during operation. Thus, in some cases it is necessary to deposit by welding a thicker layer of high alloy steel. This decision would lead to higher costs than using low alloy steel for the arc welding deposition. This paper aims to analyze this aspect and to show whether the results obtained can be extended to industrial applications.

Another aspect that needs to be taken into account is that the thermo physical properties of the two materials are different. Exposed to the same linear energy, stainless steels heat up more by the Joule-Lentz effect, which can lead to the vaporization of certain chemical constituents of the used materials. For stainless steels, this situation leads to negative consequences when using high values of arc welding deposition parameters, thus affecting productivity.

2. Input data

2.1. Base material

The base material used to deposit the seams was stainless steel X6Cr17, a ferritic magnetic stainless steel that has a low amount of carbon and chromium, between 16 and 18%. Ferritic stainless steels have good ductility properties, corrosion resistance and good workability. The microstructure can consist of ferrite (completely ferritic steels) or it can consist of ferrite with a certain percentage of martensite (semi-ferritic steels) [6]. One of the problems that might occur when welding this type of material is the increase in the grain size. In order to avoid this problem, linear energy should be maintained at low values by increasing the welding speed. Another problem affecting the results is cold cracking due to hydrogen that can be avoided by maintaining the diffusible hydrogen content at low levels. The size of the ferritic stainless steel plates used for the arc welding deposition process was 250x100x4 mm.

2.2. Filler material

The used filler material was G 42 2 M solid wire (G3Si1) with the diameter of Ø 1.2 mm; this wire is made of a low alloy steel and contains, apart from the usual chemical elements, C, P, S and Mn, respectively Si. The protective gas used during the arc welding deposition process was type M21 (Ar+18%CO_2).

According to the manufacturer, the recommended parameters for the used wire diameter are: I_s =120-330 [A], U_a = 18-30 [V] and wire feed rate v_a =2.3-13 [m/min].

2.3. Comparisons between the base and the filler material

The chemical composition of the base material and of the filler material is shown in Table 1, while Table 2 shows the mechanical characteristics of the two materials.

Table 1

Chemical composition - base material and filler material

No.	Material	Chemical element [%]*						
		C	Si	Mn	P	S	Cr	Cu
1.	Base*	0.08***	1	1	0.04***	0.015	16– 18	0
2.	Filler**	0.06 – 0.14	0.7 – 1	1.3 -1.6	0.025	0.025	0	0.3***

*values according to [13]; **values according to [14]; ***maximum values

The analysis of Table 1 shows, as far as the filler material is concerned, that:

- It has a higher C content, which leads to an increase in the hardness of the deposited material;
- It has a higher Mn content, which leads to the acceleration of the de-oxidation processes, resulting in changes to the mechanical properties of the welding seam;
- It has a low P content, which reduces the hot cracking risk;
- The Cu content in the filler material leads to higher fluidity of the liquid metal bath, which generates a better degree of admixture.

Table 2

Mechanical features – base material and filler material

No.	Material	Mechanical properties		
		R_m [Mpa]	$R_{p0.2}$ [MPa]	A [%]
1.	Base*	400-570	240-260	18-20
2.	Filler**	550-640	≥420	≥24

*according to [15]; **according to [16]; where R_m-Tensile strength; $R_{p0.2}$-0.2% yield strength; A - min. elongation at fracture.

Table 2 depicts that the filler material leads to the increase in the mechanical resistance and in the yield strength of the deposited layer.

2.4. Experimental data

2.4.1. Deposition parameters

In order to determine the relations between the geometric elements, certain properties of the deposited layers and the deposition parameters, the following values were chosen out of the direct current ranges recommended by the manufacturer:

- Deposition current: I_{s1}=160 [A]; I_{s2}=220 [A] and I_{s3}=280 [A];
- Arc voltage: U_{a1}=18 [V]; U_{a2}=22 [V] and U_{a3}=29 [V];
- Welding speed: v_{s1}=50 [cm/min]; v_{s2}=75 [cm/min].

For the pulse current the predefined parameters were:

- Deposition current, average: I_{s2}=220 [A];
- Arc voltage: U_{a1}=25 [V];
- Welding speed: v_{s1}=50 [cm/min]; v_{s2}=75 [cm/min].

By combining the above parameters, it was established that the samples should be welded with the parameters presented in Table 3.

Table 3

Predefined parameters

Sample code	I_a [A]	U_a [V]	V_s [cm/min]	Current type/ polarity
1.	160	18	50	DCEP
2.	160	18	75	DCEP
3.	280	29	50	DCEP
4.	280	29	75	DCEP
5.	220	22	50	DCEP
6.	220	22	75	DCEP
7.	220	25	50	CP
8.	220	25	75	CP

DCEP-Direct current electrode positive; CP-pulsed current

2.4.2. Determining dilution

Considering the elements shown in Fig. 1 and considering relation (1), it is possible to determine the dilution value D:

$$D = \frac{B}{A+B} x100\ [\%] \quad (1)$$

2.4.3. Experimental research procedure

2.4.3.1. Stages of the experimental research

In order to carry out the experiments, the following tasks were conducted:

- Preparing samples for the depositions with the predefined parameters;
- Arc welding deposition;
- Optical and visual examination of the resulting samples;
- Measuring the geometric elements, reinforcement (R) and seam width (W) in the areas of interest, according to Fig. 2;
- Mechanical cutting with continuous cooling, in order to prepare the metallographic samples;

- Preparing the metallographic samples in order to determine structure and hardness values;
- Microscopic examination and saving the microscopic and macroscopic images;
- Measuring hardness values in the base material, heat-affected zone and deposition;
- Using special software to measure the penetration and the areas of deposited material and base material;
- Calculating the dilution;
- Interpreting the results.

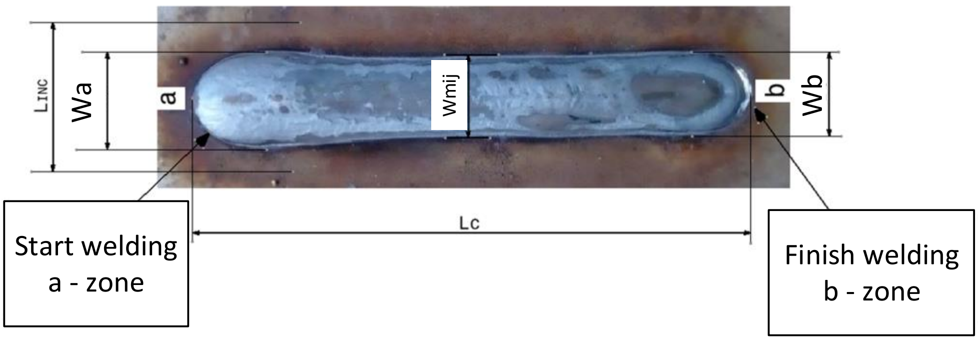

Fig. 2. Areas of interest

2.4.3.2. Equipment used for the experimental research

The main equipment/devices/tools used in the experiments are: Fanuc 1000iB Welding Robot, TRANSPULSSYNERGIC 4000 Welding Power Source, electronic calipers, hot mounting press, PHOENIX BETA Polisher, etc.

3. Results

3.1. Variation of deposit parameters

A first issue during the experiments was values of the predefined technological parameters. Even though the arc welding deposition process was robotic, during the experiments the technological parameters varied. The values recorded during the experiments are indicated in Table 4.

Table 4

Parameters recorded during the deposition

Sample code	I_{smin} [A]	I_{smax} [A]	I_{sm}** [A]	U_a [V]	v_s [cm/min]	E_l * [kJ/cm]	E_{lm} ** [kJ/cm]
1	159	161	160	17.7	50	2.7...2.74	2.72
2	157	163	160	17.7	75	1.78...1.85	1.82
3	274	288	281	29.2	50	7.68...8.07	7.88
4	279	283	281	29.2	75	5.21...5.29	5.25

5	219	223	221	21.3	50	4.5...4.54	4.52
6	218	222	221	21.3	75	2.97...3.03	3.00
7	220	224	222	24.6	50	5.2...5.29	5.25
8	220	224	222	24.6	75	3.46...3.53	3.50

I_{sm} - average value of welding deposition current; E_l - linear energy, E_{lm} - average value of linear energy * value calculated using relation (2):

$$E_l = \frac{I_s \cdot U_a}{v_s} \eta \quad \text{[J/cm]} \tag{2}$$

Where: E_l - linear energy [J/cm]; η - the value of the GMAW process efficiency (according to EN 1011-1/2009, Welding, Recommendations for welding of metallic materials. General guidance for arc welding, the η= 0.8; I_s – welding current [A]; U_a - arc voltage [V]; v_s - welding speed [cm/sec]; ** value calculated as the arithmetic mean of the minimum and maximum values.

3.2. Resulting samples

The samples obtained after the arc welding deposition process with the parameters indicated in Table 4 are shown in Fig. 3.

As it can be seen in Fig. 3, sample 3 was pierced in the end part of the deposition area due to the high linear energy generated during the arc welding deposition process. All the resulting samples were cut through the middle of the seam, perpendicular to the welding deposition direction, as one can notice in Fig. 4.

a). Sample 1 b). Sample 2 c). Sample 3 d). Sample 4

e). Sample 5 f). Sample 6 g). Sample 7 h). Sample 8

Fig.3. Experimental samples

Fig. 4. Samples cut to prepare metallographic samples

Fig. 5 illustrates several aspects that occurred during the preparation for the hot mounting process. Fig. 6 depicts metallography of the samples after mechanical and chemical processing required to highlight their micro-structure. The chemical solution used was natal consisting of nitric acid and alcohol (2.5 ml nitric acid + 100 ml alcohol). The chemical attack was carried out by immersing and shaking the sample in the reagent until the polish disappeared and the seam was highlighted. After the attack, the samples were washed in water and dried with hot air.

a) Sample 1 b) Sample 2 c) Sample 3 d) Sample 4

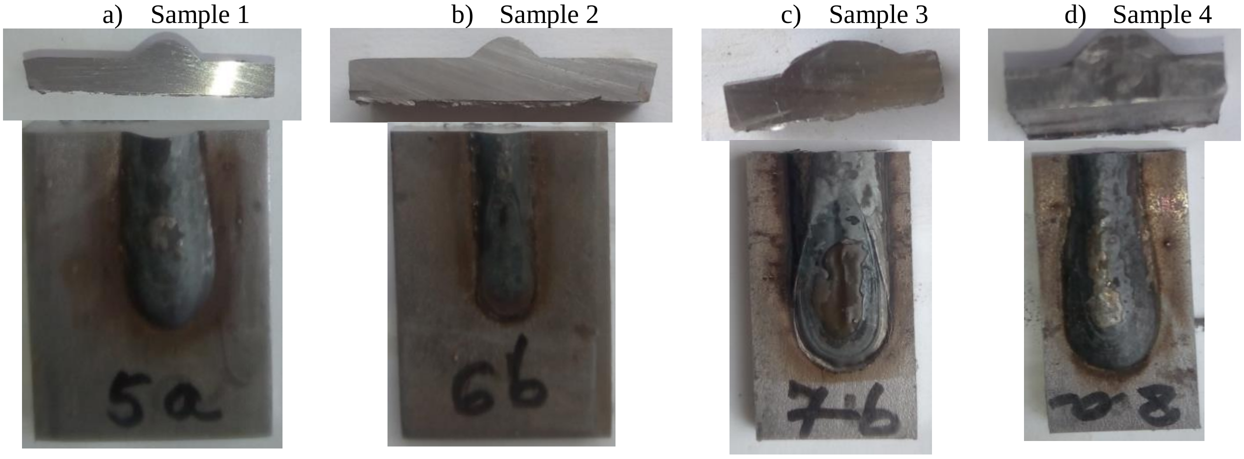

e) Sample 5 f) Sample 6 g) Sample 7 h) Sample 8

Fig. 5. Samples cut for hot mounting

Fig. 6. Metallographic samples

3.3. Measurement results

The geometric elements indicated in Fig. 2 were measured using an electronic caliper, and the results obtained are shown in Table 5.

Table 5

Measured values

Sample code	L_c [mm]*	L_{INC} [mm]**	W_{mij} [mm] ***	R_{mij} [mm]****	Area a*****		Area b*****	
					W_a [mm]	R_a [mm]	W_b [mm]	R_b [mm]
1	77.5	9.1	6.4	2	7.7	2.6	5.9	0.5
2	75.4	10.5	4.8	1.8	7.5	2.5	4.6	0.4
3	79.1	19.1	14.4	2.6	15.2	3.2	10.1	0.8
4	80.6	19.4	9.5	2.4	12.3	3	10.3	0.6
5	76.4	16.4	8.9	2.3	10.7	2.9	7.9	0.6
6	76.7	12.8	6.6	2.2	10.2	2.7	7.4	0.5
7	80	22.2	11.5	2.4	12.1	2.7	10.3	0.2
8	78.9	15.3	9.4	2.2	11.3	2.5	9.7	0.1

* L_c-total length of the seam; ** L_{INC} - heat affected zone; *** W_{mij} is the width of the seam in the middle; **** R_{mij} is the Reinforcement measured at the center of the seam; ** *** - according to Fig. 2.

The first preliminary conclusion resulting from the analysis of the results depicted in Table 5 is that the seam width decreases, regardless of the used parameters. In order to avoid this nonconformity, it is recommended to carry out the welding deposition in two adjacent passes in different ways, but with the same parameters [6]. Furthermore, the reinforcement values (R in Fig. 1) decrease in the end part of the seam due to the existence of the end welding crater. This aspect can be avoided by changing the welding deposition direction by 180 degrees on a minimum 15 mm length.

Considering the values indicated above, a series of charts were drawn to represent the variation of the geometric elements of the deposition versus the values of the welding deposition parameters. From the analysis of Fig. 7 one can conclude that when v_s = 50 cm/min, as in experiments 1, 3 and 5, the geometric elements R and W increased with the increase in the welding current value. Furthermore, the increase for the R parameter is linear. By analyzing the results depicted in Fig. 8 one can state that the geometric elements R and W increased with the increase in the welding current value when v_s = 75 cm/min, as used in experiments 2, 4 and 6.

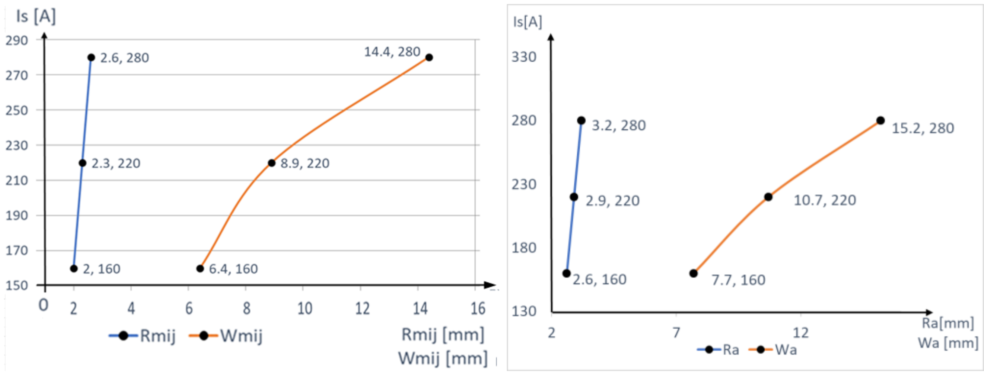

a) b)

Fig. 7. Influence of the welding current on the geometric elements R_b and Wb, I_s to v_s = 50 cm/min: R_{mij} and W_{mij} depending on the welding current value, I_s; Ra and Wa depending on the welding current value, I_s

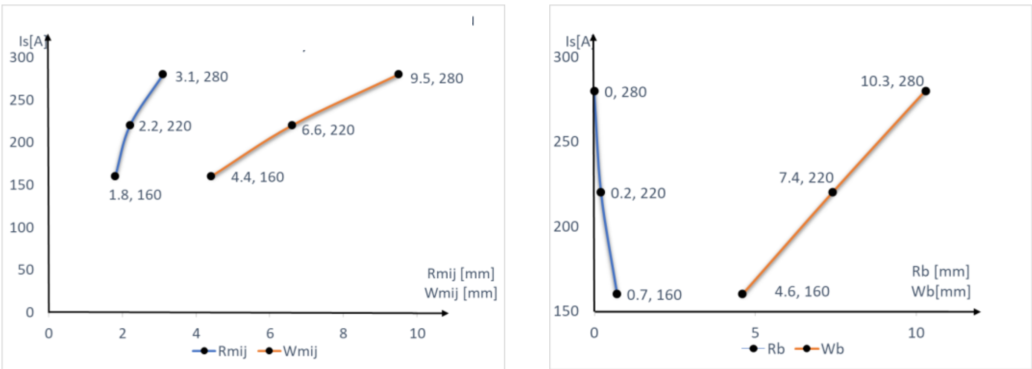

a) b)

Fig. 8. Influence of the welding current on the geometric elements R_b and W_b, I_s to v_s = 75 cm/min; a - R_{mij} and W_{mij} depending on the welding current value, I_s; b - R_b and W_b depending on the welding current value, I_s.

3.4. Hardness results

For each area of interest, the hardness values obtained as the arithmetic mean of the three measuring points (Fig. 9) are depicted in Table 6.

Table 6

Hardness values HV5 – measurements at the central area of the seam

Sample code	HV5 Hardness
1	527.56
2	504.05
3	473.56
4	521.05
5	563.74
6	510.75
7	496.31
8	560.00

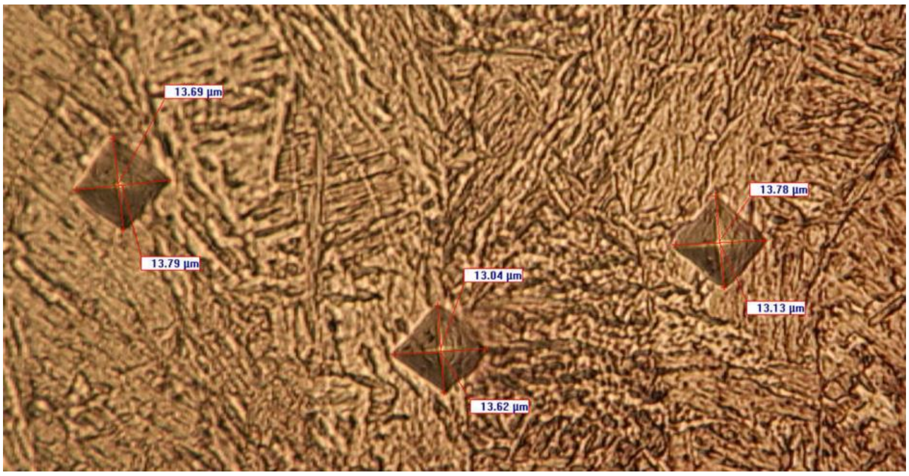

Fig. 9. Penetrating marks on sample surface

3.5. Dilution results

In order to determine the dilution values resulting from the use of various parameters, the following tasks were carried out:

- The insertion of the macro graphic image into a specialized geometric dimensioning software (Dassault SolidWorks 2018);
- The scaling of the image was performed;
- The penetration was measured, by computing area B within the outline of the seam base material and area A within the outline of the seam filler material and then applying relation 1.

The measured values for the penetration and the dilution are shown in Table 7.

Table 7

Dilution and penetration values*

Sample code	p [mm]	B [mm^2]	A [mm^2]	A_{cus} [mm^2]	D [%]
1	4	21	12.42	33.42	62.84
2	4	30.86	26.49	57.35	53.81
3	1.73	5.32	6.25	11.57	45.98
4	1.95	8.63	7.56	16.19	53.30
5	2.69	19.37	13.19	32.56	59.49
6	1.96	18.34	19.84	38.18	48.04
7	4	18.86	21.68	40.54	46.52
8	3.16	11.66	11.11	22.77	51.21

*p - penetration measured in the middle of the seam; B - the area of the base material that is involved in the seam formation; A - the area of the filler material that is involved in the seam formation; A_{cus} - total area of the deposited seam; D – dilution

The performed measurement tasks are depicted in Fig. 10.

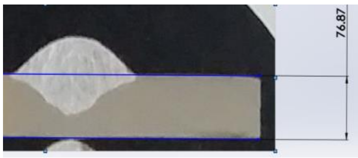

a) inserting the macroscopic image and measuring the sample thickness

b) scaling the image until the size of the base material reaches 4 mm

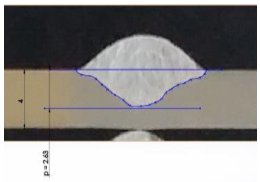

c) identifying the base material outline (B) involved in the seam formation

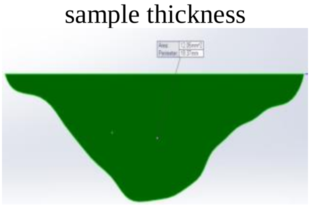

d) extracting and measuring the base material area involved in the seam formation

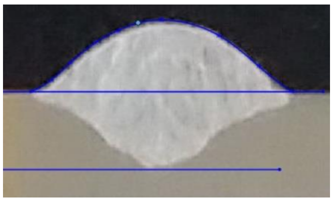

e) identifying the filler material outline (A) involved in the seam formation

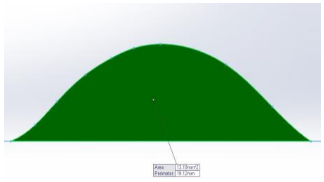

f) extracting and measuring base material area involved in the seam formation

Fig. 10. Measurement of areas and penetration using Dassault SolidWorks 2018 software application

4. Conclusions

Taking into account the above results, the following conclusions can be drawn:

- The arc welding deposition of a non-alloy filler material on a ferritic stainless-steel base material leads to acceptable results as far as the geometric configuration and the hardness of the resulted seam are concerned, when appropriate technological parameters were employed;
- The use of certain computer-aided solutions may help to determine the width, penetration and reinforcement values with high accuracy;
- The use of high linear energies - see sample 3 - may lead to the excessive penetration of the base material, thus negatively influencing the quality of the welding.
- When the deposition is performed using pulse welding current, one can obtained a similar value of the dilution (sample 7) as using direct welding current with a higher value for the linear energy (sample 3);
- The dilution value (see results in Tables 4-7) depends on the added effect of the deposition parameters.

R E F E R E N C E S

[1]. *J.R. Davis, Davis & Associates*, Stainless Steel Cladding and Weld Overlays, ASM Specialty Handbook: Stainless Steels, 06398G, pp 107 – 119.

[2]. *** http://www.polysoude.com/us/weld-overlay-cladding/, accessed on 17.02.2018.
[3]. *** http://www.esabna.com/us/en/education/blog/cladding-of-ni-alloy.cfm, accessed on 11.01.2018.
[4]. *S.H. Wang, J. Jiang, J. McKinnell*, Weld cladding for mining and mineral processing: a Canadian perspective CWA Journal, 2016, August, pp. 52-66, 2016-08-16.
[5]. *D. Capitanescu, Alloy 625 weld overlays for offshore and onshore projects, Super alloys 718,625 and Various Derivatives, Edited by Edward A. Imia, The Minerals, Metals & Materials Society, 1991*
[6]. *** EN 1011-3:2000 Welding. Recommendations for welding of metallic materials. Arc welding of stainless steels
[7]. *P. Sreeraj, T, Kannan Subhasis Majic*, Simulated annealing algorithm for optimization of welding variables for percentage of dilution and application of ANN for prediction of weld bead geometry in GMAW process., International Journal of Engineering Research and Applications (IJERA) ISSN: 2248-9622, Vol. 3, Issue 1, January -February 2013, pp.1360-1373
[8]. *J. N. DuPont,* Dilution in Fusion Welding, ASM Handbook, Volume 6A, Welding Fundamentals and Processes, pp 115 -121.
[9]. *G. Iacobescu, C. Rontescu, D.T. Cicic, C. Babis, A. Dimitrescu, O. Chivu*, Influence of the chemical composition of coated electrodes on moisture content of the coating and diffusible hydrogen in the welded metal, U.P.B. Sci. Bull., Series B, Vol. 80, Iss. 3, 2018, pp. 75-84.
[10]. *M. Besliu, I. Voiculescu, Gh. Solomon*, Effects of dilution on weld overlays realized with flux-cored arc welding (FCAW) process using 309LV filler metal on the S235JR steel, U.P.B. Sci. Bull., Series B, Vol. 79, Iss. 1, 2017, pp.173-182
[12]. *I.M. Vasile, I. Voiculescu, V. Geanta, S. Zam*fir, Some aspects regarding the microstructural and mechanical characteristics of the weld deposit on microalloyed steels for dies, U.P.B. Sci. Bull., Series B, Vol. 75, Iss. 1, 2013, pp. 209-216
[13]. *** EN 10088-2-2005, Stainless steels. Technical delivery conditions for sheet/plate and strip of corrosion resisting steels for general purposes.
[14]. *** SR EN ISO 14341: 2011 Welding consumables - Wire electrodes and weld deposits for gas shielded metal arc welding of non-alloy and fine grain steels - Classification,
[15]. *** http://www.steelnumber.com/en/steel_composition_eu.php?name_id=61, accessed on 20.01.2018.
[16].*** https://www.cemont.com/CEMONT_MIG%20MAG%20Solid%20Wire_%20 Non%20alloyed%20steel%20_STEELMIG%20G3, accessed on 20.01.2018